We thank the reviewer for the helpful and constructive feedback. We appreciate the time and effort you have dedicated to evaluating our manuscript. In the following, the comments by the reviewer (in italic blue font) are followed by our detailed responses.

The authors conducted field measurements of ambient VOC mixing ratios with a PTR-MS. They present results correlating those mixing ratios with various meteorological parameters, but this approach is fundamentally flawed. Mixing ratios are a function of emissions (source), boundary layer dynamics (dilution and transport), atmospheric chemistry (sink), and deposition (sink). They do not take any boundary layer dynamics or chemical processing into account. This can be accomplished with some supplementary modeling efforts that would help them make sense of this dataset. For example, the abstract states that "lower mixing ratios were observed around noon, suggesting inhibition of BVOC emission under the relatively high temperature and low relative humidity of drought conditions," but it is very typical for mixing ratios to decrease at the height of the day due to dilution in the growing boundary layer and increased photochemical loss processes! It doesn't necessarily tell you anything about the emissions.

Response: Based on the comments from the two reviewers, we have performed additional analyses that we believe strengthen the argument that the correlation between BVOC mixing ratios and emission rates is robust enough to support our main findings. The new analyses explore the effects of factors that could influence this correlation, including boundary layer height, photochemical loss processes, and potential contributions from outside the fetch.

Of particular importance is our finding, based on the analysis of short-lived species, that the correlation between the temporal changes in relative humidity ($\Delta RH/\Delta t$) and BVOC mixing ratios consistently increased as the potential contribution from outside the fetch decreased. Below, we summarize all the arguments that justify
the use of mixing ratios under the specific conditions of the measurements to support our analysis and findings.

1. Focusing the analyses on short-lived VOCs: In response to the reviewer's suggestion, we repeated the analysis by including only short-lived VOCs to ensure that our findings are not biased by the transport of the investigated VOCs from outside the fetch. This new analysis was based on the following two stages: i) **selection of VOCs with a short enough lifetime**. The daytime lifetimes of the various VOCs were calculated based on in situ measured O_3 mixing ratios and evaluated OH mixing ratios, using the onsite chemical and metrological conditions (Ehhalt and Rohrer (2000). Note that the resulting OH mixing ratios were in good agreement with those reported by Gabay and Tas (2019) and Gabay et al. (2020) for the same region and time during the year. Table 1 shows the resulting lifetimes for the various VOCs. In the following, "short-lived VOCs" refers to those species that, at least during part of the measurements, were not affected by emissions outside the fetch, according to our calculations. Based on these calculations, isoprene, monoterpenes (MTs) and sesquiterpenes (SQTs) were selected for further analysis as representative of short-lived VOCs. Note that due to its fast reaction with O_3, all SQT concentration data are

expected to originate from emissions within the fetch. The calculations indicate that MT and isoprene could be affected by emissions from outside the fetch during part of the time, as described in more detail below.

Table 1. *Rate constants of each VOC with OH and O_3 are presented, individually scaled on a normalized white–red scale. The lifetime range of each VOC against oxidation by OH and O_3 is also listed.*

	OH rate constant at 25°C (cm^3 $molecule^{-1}$ s^{-1})	O_3 rate constant at 25°C (cm^3 $molecule^{-1}$ s^{-1})	Lifetime against OH (s)	Lifetime against O_3 (s)
Isoprene	9.99E-11	1.28E-17	731~1820	3.3E4~8.3E4
MT *	1.36E-10	1.08E-16	537~1337	3923~9809
SQT *	2.44E-10	1.20E-14	299~745	35~88
Acetone	1.75E-13		4.2E5~1.0E6	
Acetaldehyde	1.49E-11		4.8E3~1.2E4	
MVK	1.88E-11		3.9E3~9.7E3	
Methanol	8.96E-13		8.1E4~2.0E5	
Ethanol	3.21E-12		2.3E4~5.7E4	
Formaldehyde	8.49E-12		8.6E3~2.1E4	
Acetic acid	7.40E-13		9.9E4~2.5E5	
Formic acid	4.50E-13		1.6E6~4.0E6	
DMS	4.84E-12		1.5E4~3.8E5	
H_2S	4.80E-12		1.5E4~3.8E5	
1,3-Butadiene	6.65E-11	6.33E-18	1098~2734	

ii) Evaluation **of the relative contribution of emissions from the fetch to the measured BVOCs mixing ratios**. First, we determined the distance between the fetch edge and the measurement point for each wind direction. For each time point, we calculated the travel time between the edge of the fetch and the measurement point, based on the wind speed and direction. Fig. 1 summarizes the PCA analysis previously shown in the manuscript (Fig. 6 in the manuscript) followed by a PCA for the short-lived species, MT, SQT, and isoprene (Fig. 2). The upper panel of this figure shows the same information as in Fig. 1 but only for these three species. Based on wind direction, speed, and the calculated BVOCs lifetime, the lower panels present three categories reflecting the extent to which the measured mixing ratios could be affected solely by emissions from the fetch. We have defined three categories- “60%”, “80%” and “100%” - indicating that the travel time out of the fetch was 40%, 20% and 0% of the lifetime of the species, respectively.

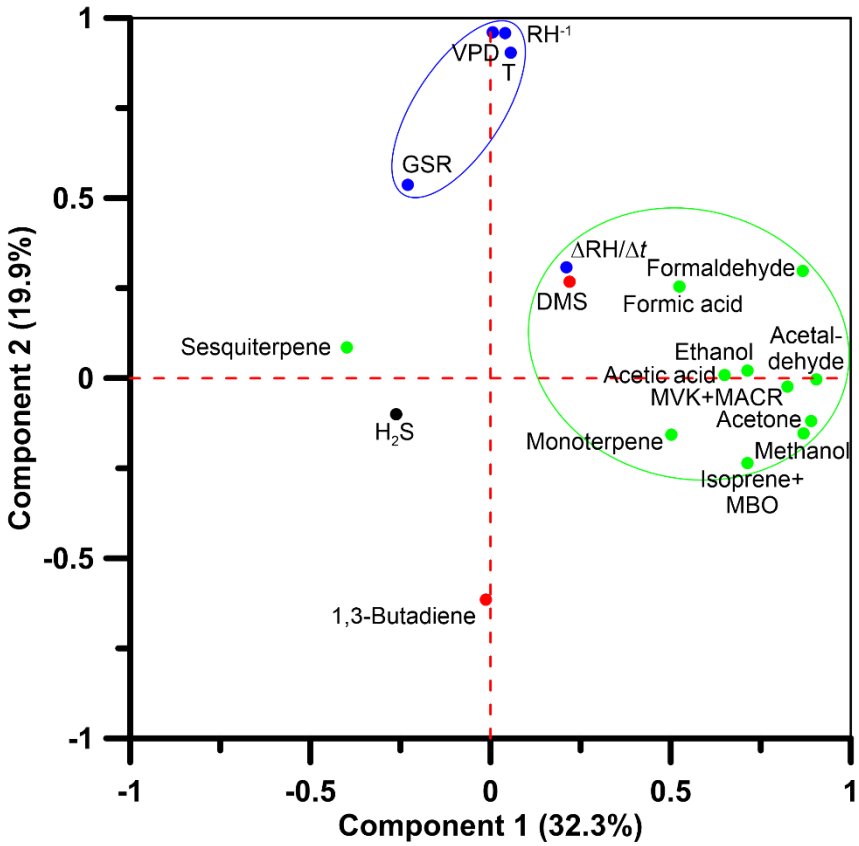

Figure 1*. *PCA of ambient meteorological parameters, including meteorological parameters and the temporal derivative of RH, and the measured mixing ratios of VOCs. Colors indicate ambient meteorological parameters (blue), BVOCs (green), AVOCs (black), and either BVOCs or AVOCs (red). Note that the inverse of RH is presented rather than RH. *identical to Fig. 6 in the main text.*

The PCA analysis presented in Fig. 2 shows similar patterns of association with the tested meteorological parameters for the short-lived BVOCs as observed for all other investigated BVOCs (Fig. 2). As mentioned in the manuscript, SQT was exceptional and showed agreement with previous studies (lines 544-548 in the manuscript; Bonn et al., 2019; Caser et al., 2019; see also Fig. 1). Fig. 2 further demonstrates a relatively strong correlation between the temporal derivative of RH (ΔRH/Δt) and component 2 along with MT and isoprene, compared to the other meteorological parameters. Moreover, the difference in correlation levels between MT, isoprene and ΔRH/Δt, consistently decreased (from 0.489 to 0.184, as indicated in the figure) when shifting from "60%" to "80%" and "100%", i.e., for reduced potential contributions from outside the fetch. This trend is indicated by the red values. This **indicates** that **as the potential for contribution from outside the fetch decreases**, the ΔRH/Δt effect plays a larger role, which **reinforces** our conclusions. This analysis will be included in the revised manuscript.

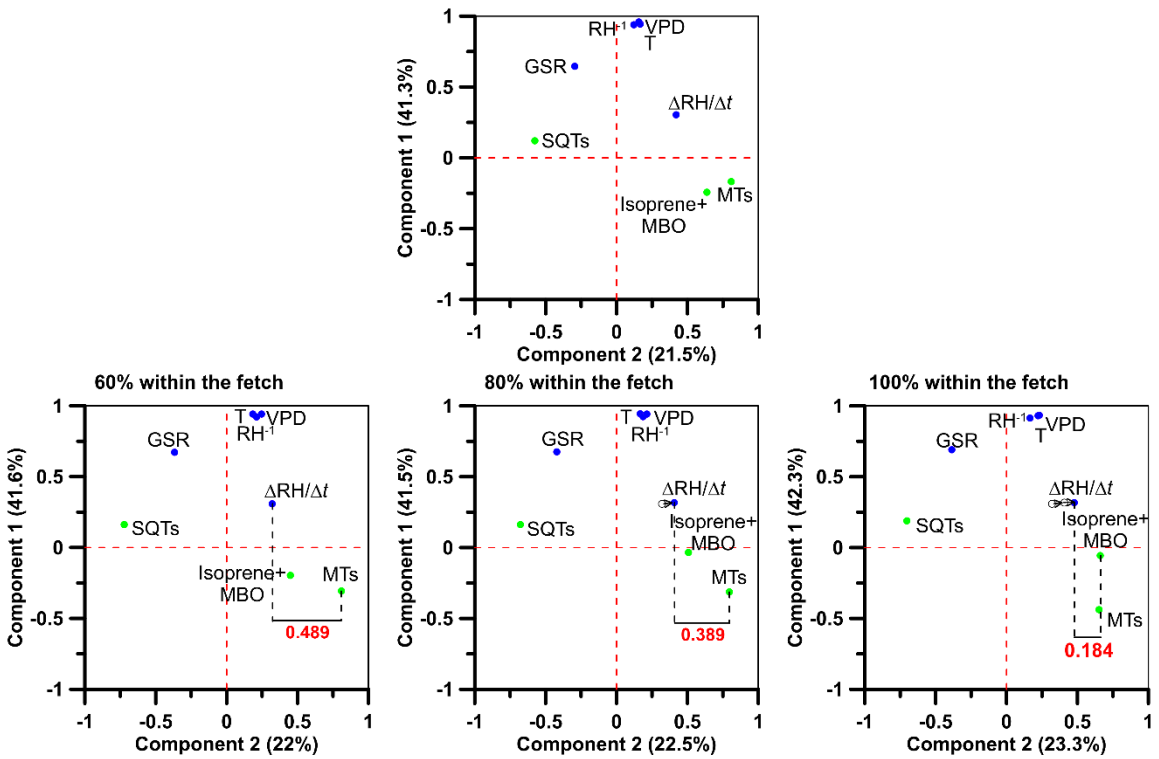

Figure 2. *PCAs of ambient meteorological parameters, including meteorological parameters and the temporal derivative of RH, and the measured mixing ratios of the short-lived BVOCs (isoprene, MTs, SQTs). The upper panel presents the PCA analysis for the full dataset including the short-lived BVOCs, while the lower three panels show the PCA analysis for different categories - "60%", "80%" and "100%" - indicating that the travel time out of the fetch was 40%, 20% and 0% of the species' lifetime, respectively.*

2. **Ruling out a potentially dominant effect of mixing height on the measured VOCs mixing ratios**: We performed model simulation using the Weather Research and Forecast (WRF) model (Skamarock et al., 2019) to simulate the planetary boundary layer height (PBLH), and thereby investigate the potential effect of changing mixing height on BVOCs mixing ratios. Version 4.2.2 was used for the simulation. The domain configuration consisted of one parent and two one-way nested grids with horizontal resolutions of 9 km (d01), 3 km (d02), and 1 km (d03), all centered over northern Israel (see Fig. 3). The set of physical parameterizations applied in this study are summarized in Table 2 and include the Yonsei University (YSU) PBL scheme (Hong et al., 2006), the Unified Noah land surface model, the Rapid Radiative Transfer Model for global circulation models (GCMs) for longwave and shortwave radiation, the Thompson microphysics scheme, the Moisture-advection-based Trigger for the Kain-Fritsch cumulus scheme (only for the d01 domain), and the Revised MM5 surface layer scheme. The modeling simulations covered the entire measurement period, including a 72-hour spin-up time. Initial and boundary meteorological conditions were obtained from the high-resolution European Centre for Medium-Range Weather Forecasts (ECMWF) Integrated Forecasting System (ISF) with a spatial resolution of 0.1° x 0.1° and a temporal resolution of 1 hour. The vertical grid was configured with 54 eta-levels, with the model top set at 5 hPa; eight of these levels are within the first kilometer above ground level (AGL) to ensure good representation of the PBL. An output temporal resolution of 15 minutes was chosen for representing PBLH.

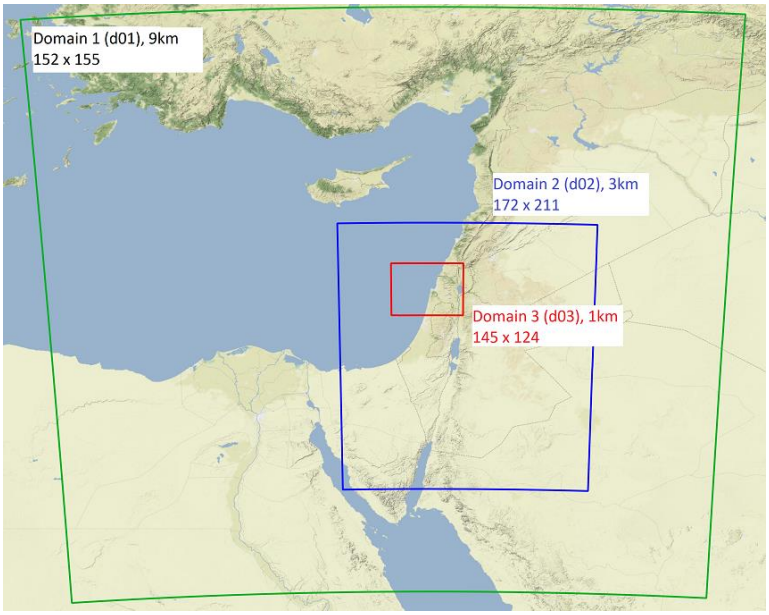

Fig. 3. *WRF Model computational domains of the simulation including three successive nested domains, centered at northern Israel with grid spacing of 9km (do1; 152x152 grid points), 3km (d02; 172x211 grid points), and 1 km (d01; 145x124 grid points).*

Table 2. *WRF parametrization schemes, used to simulate PBLH over the measurement area*

WRF namelist option	Parametrization scheme	Reference
Micro Physics Options (*mp_physics*)	Aerosol–aware & Hail/Graupel/Aerosol Thompson Schemes	(Thompson and Eidhammer, 2014)
Cumulus Parameterization Options (*cu_physics*) - only d01	Moisture–advection–based Trigger for Kain–Fritsch Cumulus Scheme	(Ma and Tan, 2009)
Shortwave (*ra_sw_physics*) and Longwave (*ra_lw_physics*) Options	RRTMG Shortwave and Longwave Schemes	(Iacono et al., 2008)
Planetary Boundary Layer (PBL) Physics Options (*bl_pbl_physics*)	Yonsei University Scheme (YSU)	(Hong et al., 2006)
Surface Layer Options (*sf_sfclay_physics*)	Revised MM5 Scheme	(Jiménez et al., 2012)
Land Surface Options (*sf_surface_physics*)	Unified Noah Land Surface Model	(Tewari, 2004)

A PCA figure including the simulated PBLH is presented below (Fig. 4). Figure 4 indicates that PBLH correlated with basic meteorological parameters and had a negligible correlation (r=-0.09) with component 1. The BVOC mixing ratios, however, showed a higher correlation with component 1. Note that while this figure indicates a relatively high correlation between $\Delta RH/\Delta t$ and BVOCs, our analysis suggests that the correlation between BVOCs and meteorological parameters should be investigated on a diurnal cycle scale (see lines 510-513, 587-595 in the manuscript). Table 3 below (similar to Table 4 in the manuscript, which is based on a daily scale analysis) indicates that on a daily basis, $\Delta RH/\Delta t$ exhibited a higher correlation with the BVOCs mixing ratios, as can be inferred from Fig. 4. Based on both Fig. 4 and Table 3, PBLH exhibited almost no correlation with the BVOCs mixing ratios. Overall, the analysis presented in Fig. 4 and Table 3 indicate

that during the daytime measurement, PBLH, as well as the absolute values of the investigated meteorological parameters, did not play a notable role in the BVOC mixing ratios. This analysis will be included in the revised manuscript.

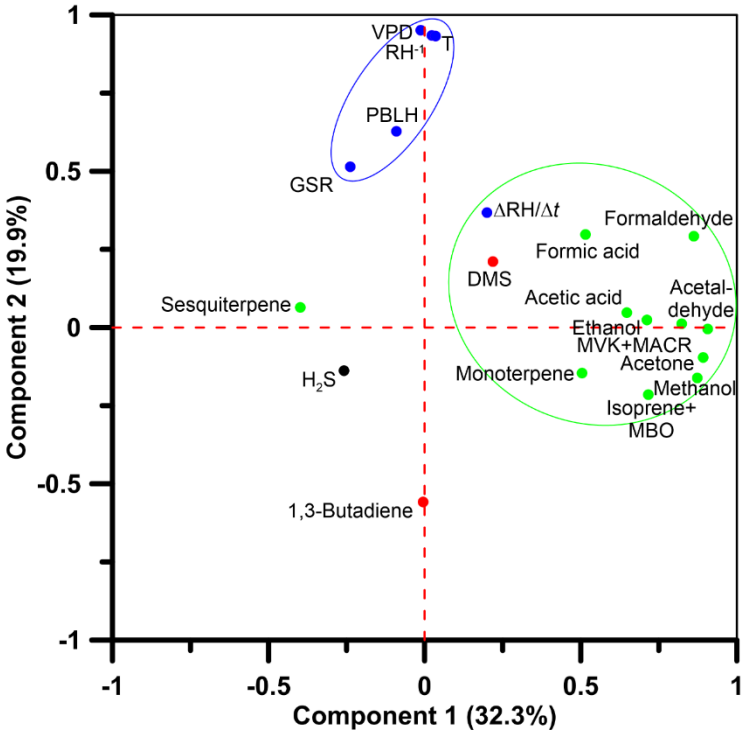

Figure 4. *PCA of ambient meteorological parameters, including meteorological parameters, planetory boundary layer height (PBLH) and the temporal derivative of RH (*ΔRH/Δt*), and the measured mixing ratios of VOCs. Colors indicate ambient meteorological parameters (blue), BVOCs (green), AVOCs (black), and either BVOCs or AVOCs (red). Note that the inverse of RH is presented rather than RH.*

Table 3. Correlation of the investigated VOCs with various meteorological parameters. Presented is the number of VOCs for which a non-statistically significant and statistically significant R with various meteorological conditions and their temporal derivatives ($\frac{\Delta T}{\Delta t}$, $\frac{\Delta RH}{\Delta t}$, $\frac{\Delta VPD}{\Delta t}$, $\frac{\Delta GSR}{\Delta t}$ and $\frac{\Delta RH}{\Delta t}$ are the temporal derivatives of T, RH, VPD, GSR and RH, respectively, and PBLH) was observed. Red and blue shading indicate positive and negative correlation, respectively. Darker color (red or blue) indicates statistically significant correlation ($P < 0.05$), while light color indicates a non-statistically significant correlation, with $0.1 > P > 0.05$.

	T	$\frac{\Delta T}{\Delta t}$	RH	$\frac{\Delta RH}{\Delta t}$	VPD	$\frac{\Delta VPD}{\Delta t}$	GSR	$\frac{\Delta GSR}{\Delta t}$	$PBLH$
DMS									
H_2S									
1,3-Butadiene									
MT									
Isoprene+MBO									
SQT									
Acetone									
Acetaldehyde									
MVK+MACR									
Methanol									
Ethanol									
Formaldehyde									
Acetic acid									
Formic acid									
	2	*6+3*	*1*	*8+2+1*	*2+1*	*8+1*	*1*	*2*	*2*

3. **The potential effect of chemical reactions on the measured VOC mixing ratios**: We calculated the lifetime of each BVOC against oxidation by O_3 or by OH (with estimated mixing ratios for OH; see Sect. 1 above) and evaluated the potential impact of these oxidation processes on the evaluated daytime drought stress index (DDSI) values, which we defined in Sect. 3.3 in the manuscript for the drought effect on BVOC mixing ratios during the daytime. The analysis indicates that chemical kinetics could contribute, on average, up to 5% to the evaluated DDSI values. Notably, DMS, monoterpenes, and sesquiterpenes exhibited chemical kinetic effects of up to 20–30% of the DDSI value. Note that H_2S exhibited a DDSI value near zero, regardless of whether its chemical oxidation was accounted for. This analysis is included in Sect. S6 of the Supplementary.

4. Distinct Correlations of BVOCs and AVOCs with instantaneous changes in meteorological conditions: Our analysis indicated a shared response of the investigated BVOCs to the meteorological parameters. The PCA analysis presented in Fig. 4 shows that all investigated BVOCs exhibit a dominant correlation with the same principal component (component 1in Fig. 4), except for SQT, which aligns with previous findings regarding SQT emission under drought conditions (lines 544-548 in the manuscript; Bonn et al., 2019; Caser et al., 2019). Similarly, Table 3 demonstrates that the temporal gradients of the meteorological parameters have a statistically significant correlation with the mixing ratios

of the vast majority of investigated BVOCs. In contrast, H_2S and 1,3-butadiene exhibited fundamentally different responses to the investigated meteorological parameters, as shown in both Fig. 4 and Table 3. These latter two compounds are expected to be emitted from anthropogenic sources, with some contributions from soil and vegetation for 1,3-butadiene (lines 415-421 in the manuscript).

Considering that the measurement of meteorological parameters was performed locally on-site and the analysis was conducted at a temporal resolution of half an hour, it is unlikely that the correlation between instantaneous changes in meteorological conditions and BVOC mixing ratios was significantly affected by the transport of VOCs from outside the fetch. This is further supported by the analysis presented above, which focuses solely on short-lived species. Moreover, the fact that the companion manuscript by Li et al. (2024) also highlights the dominant role of intraday instantaneous changes in relative humidity and temperature on BVOC emission rates, based on direct emissions measurements, suggests that the observed BVOC mixing ratios in our study effectively represent the emission rates of the investigated BVOCs.

5. **Fundamentally different responses of BVOCs vs. AVOCs to meteorological conditions:** Overall, our analysis indicates that the response of the mixing ratios of the investigated BVOCs aligns with reported patterns for the response of stomatal conductance and BVOC emission to meteorological conditions under drought. For instance, previous studies have shown that under these conditions, stomatal conductance typically demonstrates morning and afternoon peaks, associated with the so-called midday depression (e.g., Li et al., 2019; Seco et al., 2017). Fig. 4 in the manuscript clearly shows a midday depression in BVOC mixing ratios, which is not observed for H_2S—used as a reference to examine the impact of meteorological conditions on anthropogenic VOCs (AVOCs) (see also daytime drought stress index (DDSI) values in Fig. 4 in the manuscript).

6. **Similarity between BVOC emissions and their mixing ratios in previous study:** Following the reviewer's suggestion we present here a comparison of the mixing ratios of MTs with their emission rates in Birya forest, which is located about 30 km from the measurement site which was used for the current study (Shibli). This figure is taken from Seco et al. (2017). Both sites are exposed to humid Mediterranean climate conditions. While we don't have the raw data to calculate the correlation between BVOC mixing ratios and emission rates, we believe that the figure demonstrates a high correlation between MT mixing ratios and emission rates. Note that Yatir Forest is exposed to semiarid climate conditions, which are different from the conditions that the Shibli site is exposed to. We don't know of any additional study that compared BVOC mixing ratios and emission rates in the same region.

Overall, we believe that even though Fig. 5 demonstrates that the mixing ratios are affected by factors other than the BVOCs emission rates, there is a fair correlation between BVOCs emission rates and mixing ratios. Apparently, the level of correlation between BVOCs mixing ratios and emission rates in our study, was enough to reinforce the finding presented in the companion paper (Li et al., 2024) about the correlation between $\Delta RH/\Delta t$ and BVOCs emissions, based on mixing ratios.

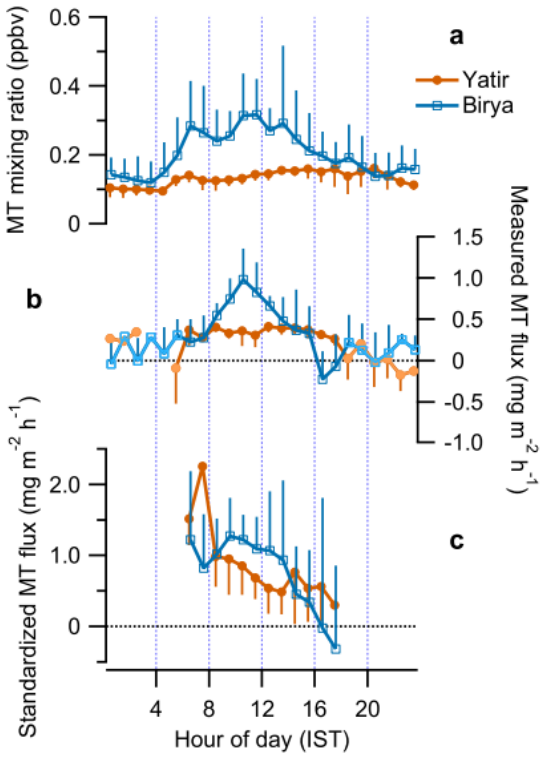

Figure. 5 *[Adapted from Seco et al. (2017)]. Hourly averaged diel cycles of the monoterpene (MT) mixing ratios (a, top panel), measured MT fluxes (b, middle panel), and standardized MT fluxes (c, bottom panel). Nighttime measured fluxes should be viewed as upper limits and are colored lighter in panel b. Standardized fluxes were computed to account for light, temperature, and tree density differences between sites and only when PAR > 150 µmol m^{-2} s^{-1}. Error bars indicate plus or minus one standard deviation for each hourly average.*

8. Similar finding based on direct BVOCs flux measurements: The fact that an independent study, described in the companion manuscript by Li et al. (2024), also indicates a dominant role of intraday instantaneous changes in relative humidity and temperature on BVOC emission rates, further suggests that the observed BVOCs mixing ratios fairly represent the emission of BVOCs from the local vegetation. Moreover, the study by Li et al. (2024) is based on direct flux measurements.

Furthermore, the data visualization was extremely difficult to interpret. I encourage the authors to think through what their main takeaway is for each figure and revise the visualization to more effectively communicate that message. They were generally too busy and appeared to be "first draft" figures without much synthesis.

Response: We will improve the quality of the figures' visualization in the revised manuscript. We believe that the figures communicate the corresponding message in the text well. We will make every effort to simplify the figures, and we would appreciate any further comments on the figure's visualization.

The manuscript was difficult to read, in part due to illogical organization. For example, they present some methods in the results section (e.g. DDSI calculations) and it is unclear what they mean by "emissions being more sensitive to intraday variation than to absolute values of met parameters." Can they provide more support for this idea?

Response: Thank you for this comment. We will attempt to make the revised version more logically organized. In particular, we believe that changing some of the section titles and including new subsections is warranted. For instance, we plan to include a subsection in Section 3.4 specifically addressing the analysis of the diurnal cycle to differentiate it from the earlier parts in Section 3.4 that present an analysis of the entire dataset.

We will include the methodological details regarding the daytime drought stress index (DDSI) in the Methods section. The sentence "…emissions, are more sensitive to intraday variations in meteorological conditions than to the absolute values of those parameters." refers to our main finding in this study, which shows that BVOC emission rates have a higher correlation with instantaneous temporal changes in meteorological parameters (e.g., $\Delta RH/\Delta t$ and temporal changes in temperature ($\Delta T/\Delta t$)) than with the absolute values of these parameters (e.g., RH and T). In the revised manuscript, we will provide additional arguments to justify using mixing ratios to support this finding, as described above.

The dominant effect of instantaneous temporal changes in meteorological parameters on BVOC emission rates is supported by Table 3. Overall, Table 3 clearly indicates that the temporal gradients of the meteorological parameters correspond with a much higher number of cases (23 out of 26) where the correlation or anticorrelation with BVOC mixing ratios was found to be statistically significant, compared to the meteorological parameters themselves (3 out of 26). Of these 23 cases, the anticorrelation of SQT with $\Delta RH/\Delta t$ is exceptional, reflecting an increase in its emission rate with increasing drought stress, in agreement with the analysis presented in Table 3 of the manuscript and in line with previous studies (lines 544-548 in the manuscript; Bonn et al., 2019; Caser et al., 2019). Table 3 suggests that under the studied conditions, $\Delta RH/\Delta t$ is the best proxy for BVOC emission under drought stress. The ranking of the various tested meteorological parameters as predictors for BVOC emission rates under drought conditions is as follows: $\Delta RH/\Delta t > \Delta VPD/\Delta t > \Delta T/\Delta t > T > VPD > \Delta GSR/\Delta t = PBLH > GSR = RH$.

The dominant effect is also supported by the figure above, which summarizes the PCA analysis for short-lived BVOCs (Fig. 2) as well as the PCA analysis for all BVOCs (Fig.4). Note that while these two figures indicate a relatively high correlation between $\Delta RH/\Delta t$ and BVOCs, our analysis suggests that the correlation between BVOCs and meteorological parameters should be investigated on a diurnal cycle scale (see lines 510-513, 587-595 in the manuscript). Therefore, we believe that the analysis presented in Table 3 is more representative of the dominant effect of instantaneous changes in meteorological conditions on BVOCs emission rates.

The abstract abruptly ends with a statement about biogenic sources of 1,3-butadiene that did not logically flow from any of the previous sentences.

Response: We have revised the sentence as follows: "Finally, while 1,3-butadiene is frequently used as a proxy for anthropogenic emissions, our analyses provide strong evidence that 1,3-butadiene is emitted by biogenic source, consistent with findings of few other studies."

The authors should also be careful about using a PTR to quantitatively measure formaldehyde. This is very difficult to accomplish since formaldehyde has a proton affinity just slightly higher than water and therefore the back-reaction can (and does) occur. The formaldehyde sensitivity of the instrument is therefore a function of humidity. I didn't see any discussion of this in the manuscript, but apologies if I just missed it.

Response: The calibration of the Proton Transfer Time-of-Flight Mass Spectrometer (PTR-ToF-MS) was performed every 3 hours, which is expected to address the potential effect of changes in relative humidity on the measured formaldehyde mixing ratios. We will include a brief discussion on the sensitivity of formaldehyde measurement to relative humidity in Sect. 2.2, explaining how our frequent calibrations account for this effect.

The dataset is interesting and valuable, but the authors need to take some more time making sense of it. Measurements of ambient mixing ratios are not the same as "emissions" or "fluxes" and the synthesis will require more supplemental modeling to get there.

Response: Thank you for your comments. We hope that our revisions adequately address the issues raised by the reviewer.

References

Bonn B., Magh R.-K., Rombach J., Kreuzwieser J., 2019. Biogenic isoprenoid emissions under drought stress: Different responses for isoprene and terpenes. Biogeosciences 16(23),4627–4645. https://doi.org/10.5194/bg-16-4627-2019.

Caser M., Chitarra W., D'Angiolillo F., Perrone I., Demasi S., Lovisolo C., Pistelli L., Pistelli L., Scariot V., 2019. Drought stress adaptation modulates plant secondary metabolite production in Salvia dolomitica Codd. Industrial Crops and Products 129,85–96. https://doi.org/10.1016/j.indcrop.2018.11.068.

Ehhalt D.H., Rohrer F., 2000. Dependence of the OH concentration on solar UV. J. Geophys. Res. 105(D3),3565–3571. https://doi.org/10.1029/1999JD901070.

Gabay M., Raveh-Rubin S., Peleg M., Fredj E., Tas E., 2020. Is oxidation of atmospheric mercury controlled by different mechanisms in the polluted continental boundary layer vs. remote marine boundary layer? Environ. Res. Lett. 15(6),64026. https://doi.org/10.1088/1748-9326/ab7b26.

Gabay M., Tas E., 2019. Dispersion-box modeling investigation of the influences of gasoline, diesel, M85 and E85 vehicle exhaust emission on photochemistry. Environmental pollution (Barking, Essex 1987) 252(Pt B),1863–1871. https://doi.org/10.1016/j.envpol.2019.05.142.

Hong S.-Y., Noh Y., Dudhia J., 2006. A New Vertical Diffusion Package with an Explicit Treatment of Entrainment Processes. Monthly Weather Review 134(9),2318–2341. https://doi.org/10.1175/MWR3199.1.

Iacono M.J., Delamere J.S., Mlawer E.J., Shephard M.W., Clough S.A., Collins W.D., 2008. Radiative forcing by long-lived greenhouse gases: Calculations with the AER radiative transfer models. J. Geophys. Res. 113(D13),19. https://doi.org/10.1029/2008JD009944.

Jiménez P.A., Dudhia J., González-Rouco J.F., Navarro J., Montávez J.P., García-Bustamante E., 2012. A Revised Scheme for the WRF Surface Layer Formulation. Monthly Weather Review 140(3),898–918. https://doi.org/10.1175/MWR-D-11-00056.1.

Li Q., Gabay M., Rubin Y., Raveh-Rubin S., Rohatyn S., Tatarinov F., Rotenberg E., Ramati E., Dicken U., Preisler Y., Fredj E., Yakir D., Tas E., 2019. Investigation of ozone deposition to vegetation under warm and dry conditions near the Eastern Mediterranean coast. Science of The Total Environment 658,1316–1333. https://doi.org/10.1016/j.scitotenv.2018.12.272.

Li Q., Lerner G., Bar E., Lewinsohn E., Tas E., 2024. Impact of meteorological conditions on BVOC emission rate from Eastern Mediterranean vegetation under drought. Biogeosciences. https://doi.org/10.5194/egusphere-2024-529.

Ma L.-M., Tan Z.-M., 2009. Improving the behavior of the cumulus parameterization for tropical cyclone prediction: Convection trigger. Atmospheric Research 92(2),190–211. https://doi.org/10.1016/j.atmosres.2008.09.022.

Seco R., Karl T., Turnipseed A., Greenberg J., Guenther A., Llusia J., Peñuelas J., Dicken U., Rotenberg E., Kim S., Yakir D., 2017. Springtime ecosystem-scale monoterpene fluxes from Mediterranean pine forests across a precipitation gradient. Agricultural and Forest Meteorology 237-238,150–159. https://doi.org/10.1016/j.agrformet.2017.02.007.

Skamarock W.C., Klemp J.B., Dudhia J., Gill D.O., Liu Z., Berner J., Wang W., Powers J.G., Duda M.G., Barker D.M., others, 2019. A description of the advanced research WRF version 4. NCAR tech. note ncar/tn-556+ str 145.

Tewari M., 2004. Implementation and verification of the unified NOAH land surface model in the WRF model. 20th conference on weather analysis and forecasting/16th conference on numerical weather prediction,11–15.

Thompson G., Eidhammer T., 2014. A Study of Aerosol Impacts on Clouds and Precipitation Development in a Large Winter Cyclone. Journal of the Atmospheric Sciences 71(10),3636–3658. https://doi.org/10.1175/JAS-D-13-0305.1.